Korean J. Chem. Eng., **27**(3), 874-880 (2010)
DOI: 10.1007/s11814-010-0144-4

Evaluation of the effect of baffle shape in flocculation basin on hydrodynamic behavior using computational fluid dynamics

Youngman Cho*,†, Soojeon Yoo*, Pyeongjong Yoo*, and Changweon Kim**

*Water Quality Research of Busan Water Authority, Gimhae, Gyeongnam 621-813, Korea
**Department of Environment Engineering, Pusan National University, Busan 609-735, Korea
(*Received 27 April 2009 • accepted 13 October 2009*)

Abstract−This study on the party wall of a flocculation basin provides important ground to facilitate the inducement of uniformity in the rectangular sedimentation basin and to achieve an improvement in sedimentation efficiency. In the water treatment plant used for this study, perforated baffle type, square type, pillar type and downward rectangular type partitions have been applied. We evaluated the hydrodynamic behavior of several types of party walls in the flocculation basin by using computational fluid dynamics (CFD). The perforated baffle type demonstrates more effective output for uniform flow than the square type, and the third party wall of the flocculation process has the most influence of the three party walls for water flow distribution. To prevent sinking of the flocs formed between the third party wall and the final outlet wall, it is necessary to develop the third party wall into an actual final outlet wall or to modify it into a pillar baffle type. In the case of a drinking water treatment system that treats low density water, a perforated baffle is more efficient as the final outlet wall because a downward rectangular type may form a bottom flow, which may cause a reduction in the efficiency of the volume capacity.

Key words: Flocculation, Party Walls, Perforated Baffle, Computational Fluid Dynamics (CFD)

INTRODUCTION

Flocculation is the gentle mixing phase that follows the rapid dispersion of coagulant by the flash mixing unit. Its purpose is to accelerate the rate of particle collisions, causing the agglomeration of electrolytically destabilized colloidal particles into settleable and filterable sizes. Flocculation basins are frequently designed to provide for tapered flocculation in which the flow is subjected to decreasing velocity gradient (G) values as it passes through the flocculation basin. Typical arrangements for flocculators are paddle wheels on horizontal shafts, while at least three consecutive compartments are required to minimize short circuiting. Though the compartments are separated by perforated baffle, the flow of the flocculation basin is a non-uniform flow. Its flow therefore affects the efficiency of sedimentation [1]. The efficiency of sedimentation is affected by the inlet energy, turbidity, water temperature, and weather conditions. The inlet kinetic energy is the most important factor among the influence items [2]. However, the inlet kinetic energy is affected by the shape and composition of the party wall in the flocculation basin used for the partitions between compartments [3]. The study on the party wall of a flocculation basin is very important to facilitate an inducement of uniformity in the rectangular sedimentation basin and to achieve an improvement in sedimentation efficiency.

In general, the party wall of a flocculation basin and the inlet wall of a sedimentation basin are of a perforated baffle type. In some cases, a square type of partition has been applied in flocculation basins, but at the water treatment plants targeted in this study, several types of party walls have been applied as partitions, such as perforated baffle, square, pillar and downward rectangular. In particular, the downward rectangular type is very rare in water treatment plants because it is encouraged to only be used for treatment of wastewater with a high turbidity. The turbidity of waste water is higher than that of tap water. Therefore, the low positioning of inlets reduces the density current and improves settling efficiency [4]. However, a density current does not frequently occur and is not strong in water treatment. We therefore need to assess the reasonableness of a downward rectangular type of party wall as well as several other types in the process of water treatment.

For the evaluation of hydrodynamic behavior in the water treatment process, a tracer test is frequently used, but it can be costly and time-consuming, especially if a variety of flow conditions and geometric variations are considered. Due to the convenience of increasingly faster digital computers and the efficient implementation of accurate numerical algorithms, computational fluid dynamics (CFD) is a valuable tool for quickly extracting accurate information about turbulent flow and mixing in industrially relevant devices in which complex geometries would have prevented modeling just a few years ago [5,6]. Recently, CFD has been accepted as a useful tool for the modeling of water treatment systems [2]. We therefore conducted a CFD simulation for an evaluation of hydrodynamic behavior in a flocculation basin.

As aforementioned, in the water treatment plant used for this study, perforated baffle type, square type, pillar type and downward rectangular type partitions have been applied. In this study, we evaluated the hydrodynamic behavior of several types of party walls in the flocculation basin using the Computational Fluid Dynamics (CFD).

MATERIALS AND METHODS

The samples of water treatment plants referenced in this study have been taken from the Nakdong River, which is located in Busan,

†To whom correspondence should be addressed.
E-mail: cho1221@korea.kr

Table 1. Operating parameter of flocculation basin

Items	Operation parameter
Basin size	B12 m×L14.4 m×H4.0 m
HRT	50 min,
Flocculator	paddle wheels on horizontal shafts (3 step)
Spin	1, 2 step clockwise.
Direction	3 step counterclockwise

Table 2. The compositions of partition wall type

Step case	1 step	2 step	3 step	4 step
1	P.B	P.B	P.B	D.R
2	S	S	P.B	D.R
3	S	S	P	D.R
4	S	S	P	P.B
5	P.B	P.B	P.B	P.B
6	PB	P.B	P	P.B

P: Pillar, S: Square, P.B: Perforated baffle, D.R: Downward rectangular

Korea. One of the two plants has fourteen flocculation basins and the other has eight. The flocculation terms are presented in Table 1. The shapes of the partition walls are schematically shown in Fig. 1, and the compositions of the walls are shown in Table 2. Cases 1, 2, 3 and 5 are real plant compositions and cases 4 and 6 are theoretical cases for comparison with the real plants. The outlet wall type of cases 1, 2 and 3 is the downward rectangular type, and the outlet wall type of cases 4, 5 and 6 is the perforated baffle type.

The ratio of the orifice area of perforated baffle to the cross-sectional area of the baffle is 6% and the square type is the same, but the downward rectangular type is 34%. The orifice diameter of perforated baffle is 10 mm. The size of downward rectangular type is 0.8 m×4.5 m×2 (Length×Width), 0.7 m×4.5 m×2 (Length×Width), 0.5 m×4.5 m×2 (Length×Width). The size of square type and pillar type is 2 m×2 m (Length×Width), 0.3 m×0.3 m×4 m×5 (Length×Width×Height), respectively. For the evaluation of the output pattern, we assigned a number to each outlet of the downward rectangular type (Fig. 1(a)) and subdivided the perforated baffle into six groups such as the top part (left, right), middle part (left, right) and bottom part (left, right) which divides equally at the outlet baffle in the vertical and horizontality direction (Fig. 1(b)).

The reliability and accuracy of CFD simulation was investigated by comparison with experimental data of case 2. We used sodium fluoride for the tracer test. After the sodium fluoride was dissolved in water, it was rapidly poured at the inlet of the flocculation basin. We sampled the output water at 5-minute intervals at the outlet of the flocculation basin and measured the fluoride ion concentration by ion chromatography. The sampling port was fifty centimeters in front of the outlet wall and one meter under the water surface and from the side wall.

SIMULATION

In the late 1970s, the development and availability of new high speed computers and new computational techniques made it possible to numerically compute the basic Navier-Stokes equation [5]. Typically, the K-Epsilon model has been applied for the CFD simulation of water treatment flow [7,16,17]. An immediate benefit of the realizable K-Epsilon model is that it more accurately predicts the spreading rate of both planar and round jets. It is also likely to provide superior performance for flows involving rotation, boundary layers under strong adverse pressure gradients, separation, and recirculation [8-10].

In this present study, the model development and simulation were based on commercial CFD software, Fluent 6.3, and meshing software Gambit 2.4 (Fluent Inc., NH, USA). Fluent 6.3, which is a finite-volume code, was used in hydrodynamics and mass transfer computations, while Gambit 2.4 provided complete mesh flexibility in solving flow problems with both structured and unstructured meshes [10,11].

The governing equations based on the continuity are the equations of momentum conservation of the Navier-Stokes Equation. The assumptions used for solving the above equations included: (1) steady state operation; (2) turbulent flow regime (Realizable k-epsilon) and (3) Non-slip boundary conditions at wall surfaces. The boundary conditions of the inlet and outlet were velocity inlet and pressure outlet, respectively. The flocculator spin was multiple rotat-

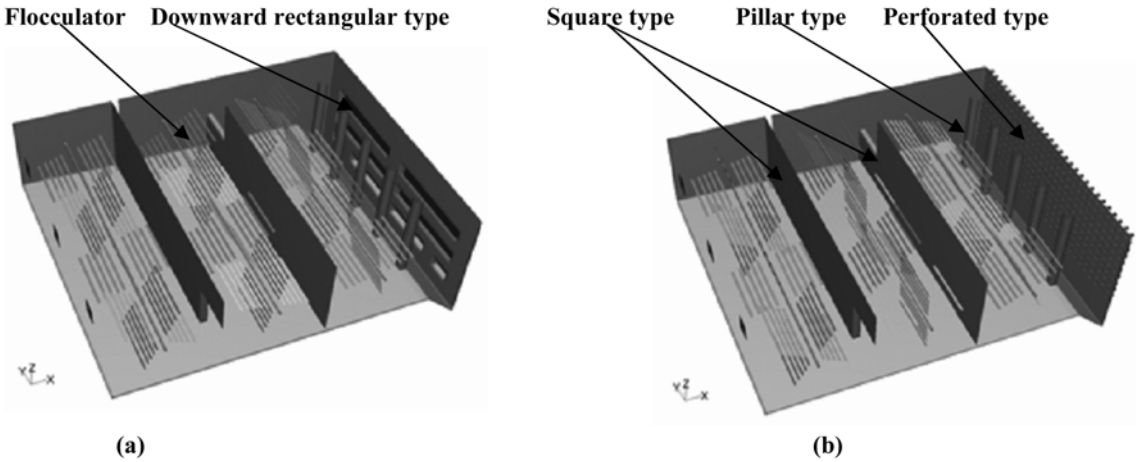

Fig. 1. The partitions wall type in the flocculation basin: (a) Case 3, (b) Case 4.

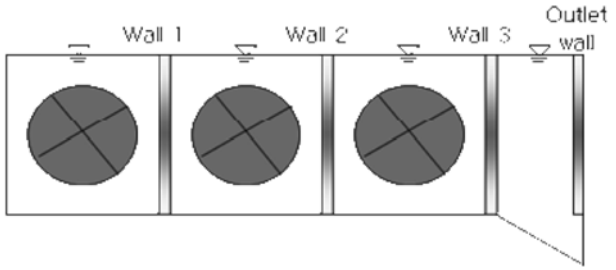

Fig. 2. A cross section of flocculation basin.

ing reference frames (MRF) at the motion type in the boundary condition. Hence, MRF approaches can be assumed as steady-state approximations and the sliding mesh model approaches, on the other hand, inherently unsteady state due to the motion of the mesh with time. The MRF approach was found to be sufficient to develop an understanding of the magnitude of velocity gradients to which a floc may be subjected within a vessel [12]. The dimension of simulation shown in 3D and the limits of simulation in this paper were applied as Fig. 2. The geometry for each wall type was drawn by method of copy, paste and split in Gambit.

We used the species transport method in Fluent for the evaluation of hydrodynamic behavior. This method can be used to model the mixing and transport of chemical species by solving conservation equations describing convection, diffusion, and reaction sources for each component species. The FLUENT predicts the local mass fraction of each species, Yi, through the solution of a convection-diffusion equation for the ith species. The species equation is the same as Eq. (1). Here, Yi is the local mass fraction and Ji is the diffusion flux of species I [9].

$$\frac{\partial}{\partial t}(\rho Yi) + \nabla(\rho \vec{v} Yi) = -\nabla(\vec{Ji}) \quad (1)$$

The species transport method in Fluent is similar to the method used in the trace test. After the simulation of the flow and turbulence in the steady state is finished, under the results, the species transport is simulated in the unsteady state. The detailed procedure of methodology begins with that we selected water as a chemical species. First, the species (water) was poured into the inlet port for five seconds. Second, the concentration of output was collected at the outlet every 0.5 second.

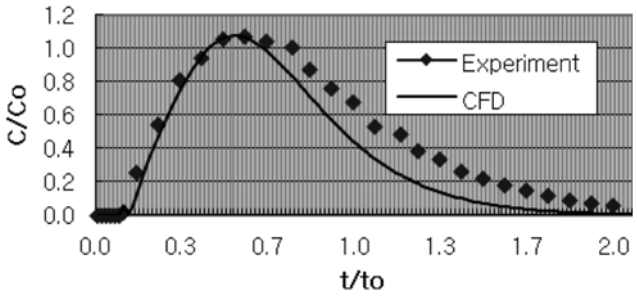

Fig. 3. Comparison of CFD simulation and experimental data (C and Co is effluent concentration and total concentration, respectively, t is effluent time of species, t0 is hydraulic retention time.

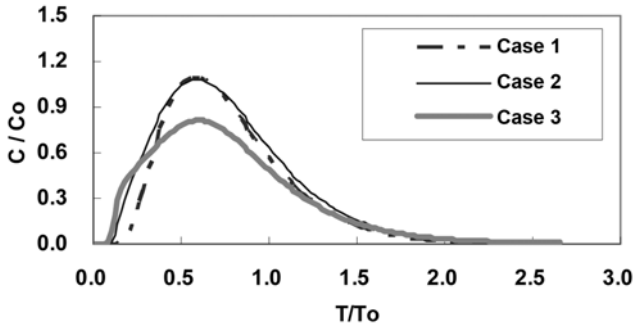

Fig. 4. Total effluent concentrations of cases 1, 2, 3.

RESULTS AND DISCUSSION

1. Comparison of CFD Simulation and Experimental Results

The reliability and accuracy of CFD simulation was investigated by comparison with experimental data of case 2 (Fig. 3). Total concentration demonstrated in Fig. 3 is a value dividing total amount of the influent tracer (sodium fluoride) by volume of flocculation basin. The recovery ratio of fluoride ion was 96% in the tracer test. The result data showed an almost similar trend to both the CFD simulation and the experimental data. The start and maximum points are the same. However, for the CFD simulation data, the concentration was reduced more rapidly than that of the experimental data after the maximum point was reached. This result is similar to that obtained from previous investigations [13].

2. Flow Characteristics According to Party Wall Type

The main aim of species test simulation is to evaluate the flow characteristics of cases 1, 2 and 3. The total concentrations of the species as a result of simulation are collected at the outlet of the flocculation process, and are shown in Fig. 4. In Fig. 4, first, the concentration profile of case 1, which consists of three perforated baffles as the first, second and third party walls, is a typical parabola shape. Second, case 2, which consists of a square type as the first and second party walls and a perforated baffle type as the third party wall, has a similar concentration profile as that of case 1, while the initial time is 5 minutes faster than that of case 1. Finally, the result profile of case 3, which consists of a square type as the first and second party walls and a pillar type as the third party wall, is a skewed parabola shape, and the initial time is one minute faster than that of case 2. For these reasons, we can suggest that the square type party wall is less effective in terms of uniformity compared with the perforated baffle. In addition, by comparing the results of case 2 and case 3, we can deduce that the concentration profile is more affected by the third party wall than by the first or second party wall.

Originally, the purpose of using the square type as a party wall is to extend the flow time by widening the distance between the inlet and the outlet and to lead the plug flow by applying the concept of "First in, First out". Although the LW ratio for an ideal plug flow ranges from 16 to 20, the length/width ratio of the flocculation basin targeted in this study is less than 3, and the mixing caused by the flocculator renders it difficult to lead the plug flow of the flocculation process [14]. Thus, flow via the square type party wall is less effective for uniformity, and the initial time is faster compared to that of flow via the perforated baffle.

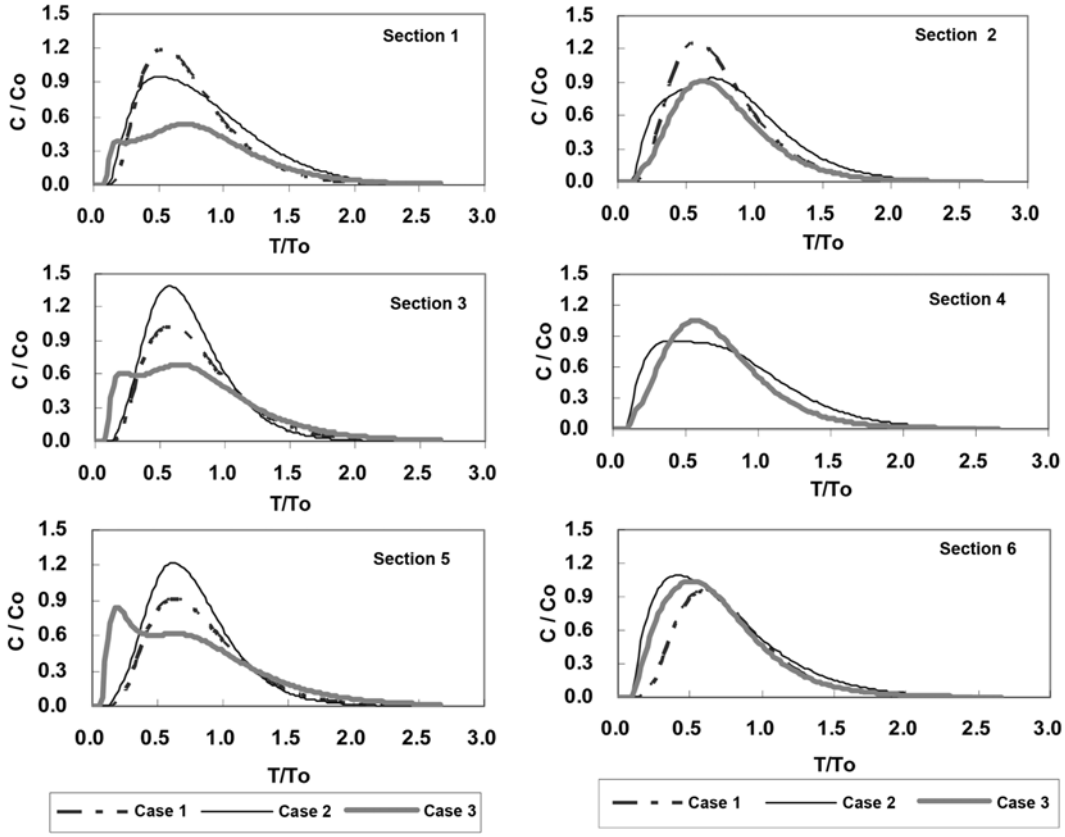

Fig. 5. Effluent concentration at the each sections of case 1, 2 and 3: Sections 1, 2, 3, 4, 5, 6.

As mentioned in chapter 2, we separated the outlet into six sections. Fig. 5 indicates the concentration profile of the outlet that is divided into the six sections of case 1, case 2, and case 3. The position of the six sections is shown in Fig. 1(a). In contrast to case 1, which has a concentration profile shaped like a typical parabola, the concentration profiles of cases 2 and 3 are skewed parabola shapes. Sections 1, 3, and 5 included in the outlet of case 3 have a particularly twisted concentration profile, due to the eddies and dead spaces formed in the direction of sections 1, 3, and 5, which are farther away from the outlet of the second square type party wall.

Similar results are also found from the effluent rate percentage of the six sections as demonstrated in Table 3. In cases 1 and 2, the effluent of each section varies in proportion to a top, middle, and bottom opening ratio (respectively 14%, 13%, and 8%), because the flow nearby the outlet is distributed uniformly through the perforated baffle as the third party wall. Conversely, the result of case 3 is in discord with the opening ratio since the effluent of the middle section is the maximum value.

Table 3. Effluent flux (%) at the top, middle and bottom of cases 1, 2, 3

Section case	Top		Middle		Bottom	
	1	2	3	4	5	6
Case 1	21.0	21.6	16.1	16.4	12.4	12.5
Case 2	24.0	24.7	18.8	19.0	7.1	6.5
Case 3	16.3	14.3	20.0	18.9	14.4	16.2

Fig. 6 provides the simulation results of cases 4, 5 and 6, which have a perforated baffle as a final outlet. First, the concentration profile of case 4, which has a square type as the first and second party walls, is a skewed parabola shape and the initial time is 2 minutes faster than that of cases 2, 5 and 6. In contrast to case 4, the concentration profile of cases 5 and 6, which have a perforated baffle as the first and second party wall, is a typical parabola shape. When considering these results, we can potentially conclude that the square type party wall has an adverse condition for uniform flow, including eddies and short-circuiting flow, compared to the perforated baffle type. These results can also be explained by adopting the magnitude of velocity vector and the turbulent dissipation rate as indicated in Fig. 7 and Fig. 8. Fig. 8 provides the turbulent dissipation rate of cases 4, 5 at the space between the third wall and outlet wall (X= 6 m, Z=1 m; 1 m under the water surface, Y=−6 m~6 m). Floc size

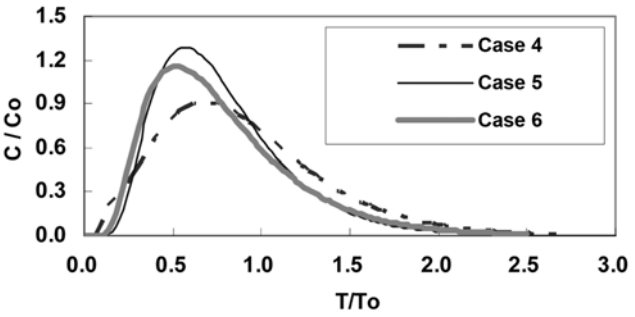

Fig. 6. Total effluent concentrations of cases 4, 5, 6.

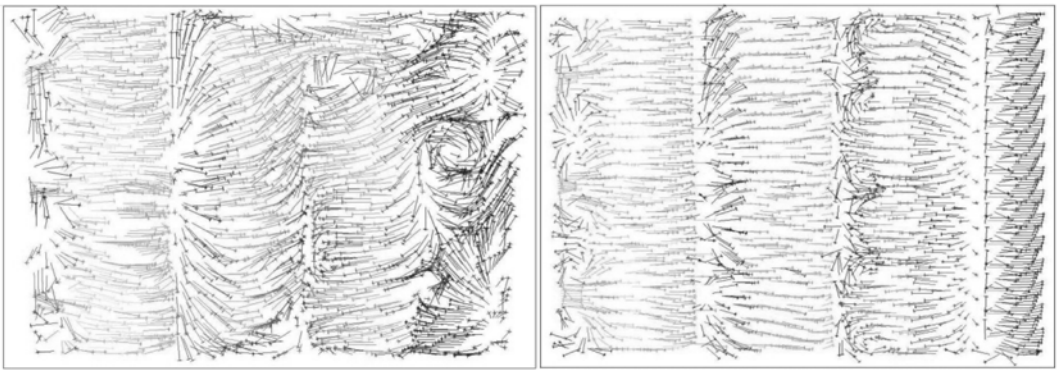

Fig. 7. Plane figure (1 m under the water surface) of the velocity vector of cases 4, 5: (a) Case 4, (b) Case 5.

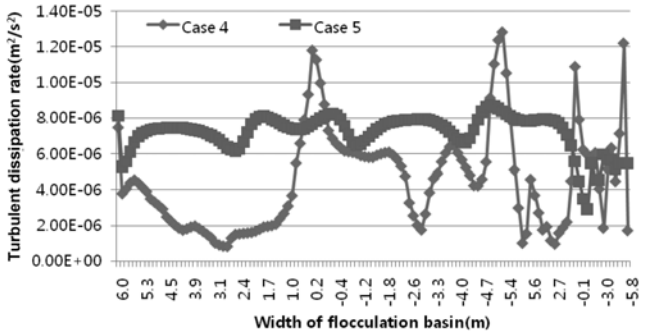

Fig. 8. Turbulent dissipation rate (Epsilon) of case 4 and case 5 (X= 6 m, Z=1 m, Y=−6 m~6 m).

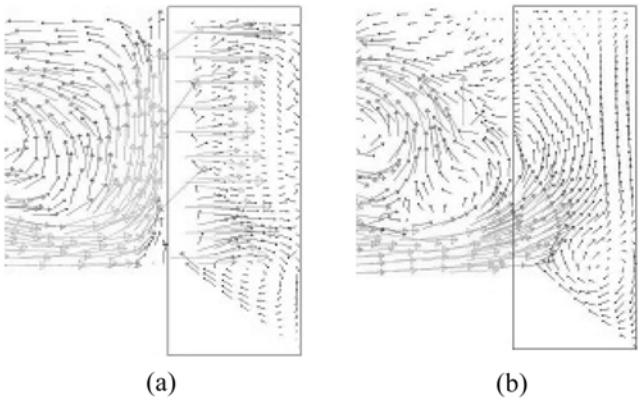

Fig. 9. A sectional view of the velocity vector at space between the third wall and outet wall in cases 5, 6: (a) Case 5, (b) Case 6.

may be considered to be a balance between the hydrodynamic forces exerted on a floc and the strength of the floc. Where the floc strength is resistant to the hydrodynamic forces, one would expect floc size either to remain constant or for growth to occur. Where the hydrodynamic forces exceed floc strength, breakage will occur.

$$B=\text{Hydrodynamic forces/Floc Strength}=F/J \quad (2)$$

Where F represents the hydrodynamic forces exerted by the flow and J represents the strength of the floc. It is clear from Eq. (2) that breakage will occur when B>1 and floc size will be maintained or increased when B<1. Floc strength, J is a function of the physico-chemical conditions (raw water type, coagulant type and dose) and the floc structure. Hydrodynamic force, F is dependent on the turbulence dissipation rate and floc strength, irrespective of sub-range. F may be expressed as:

$$F=C_2\rho\varepsilon^{2/3}d^{8/3} \quad (3)$$

Where C_2 is a constant and d is the floc diameter. So floc breakage is influenced by the turbulence dissipation rate [15]. Therefore, Fig. 8 indicates that the floc breakage possibility of case 4 is high cases 5, 6 are almost the same concentration profile (Fig. 6). The third wall of cases 5, 6 is a perforated baffle and the pillar type, respectively. In case 5, the rotational effects of flocculator have no effect on the space between the third wall and outlet wall. The velocity vector is shown in Fig. 9(a). So the formed flocs are settled at the space in a real water treatment process. But in case 6, the rotational effects of flocculator have an effect on space between the third wall and outlet wall because the third wall is pillar type. The velocity vector is shown in Fig. 9(b). So the formed flocs are not settled. Therefore, case 6 is better than case 5.

Fig. 10 shows the concentration profile of the outlet for cases 4, 5 and 6 which are subcategorized into six sections. While cases 5 and 6, which have a concentration profile shaped like a typical parabola, the concentration profile of case 4 is a skewed parabola shape. In particular, sections 1, 3 and 5 that are included in the outlet of case 4 have a twisted concentration profile. These results suggest that eddies and dead spaces are formed in the direction of sections 1, 3 and 5, which are some distance from the outlet of the second square type party wall. This is the cause of delay in the peak time at case 4 in Fig. 6. The effluent rate percentages of the six sections of the outlet are indicated in Table 4. In cases 4, 5 and 6, the effluent percentage of each section shows similar numerical values through the entire outlet. The kinetic energy of flow, which is formed when passing by the first and second party walls, decreases significantly, passing without resistance through the pillar and perforated baffle as the third party wall. Therefore, it can be concluded that the outlet percentage of each section shows a similar numerical value through the entire outlet.

Indexes for evaluating the mixing level are revealed in Table 5. For the T10 index indicating the initial time, in the cases 2, 3 and 4, which include square type party walls, the values of T10 are lower

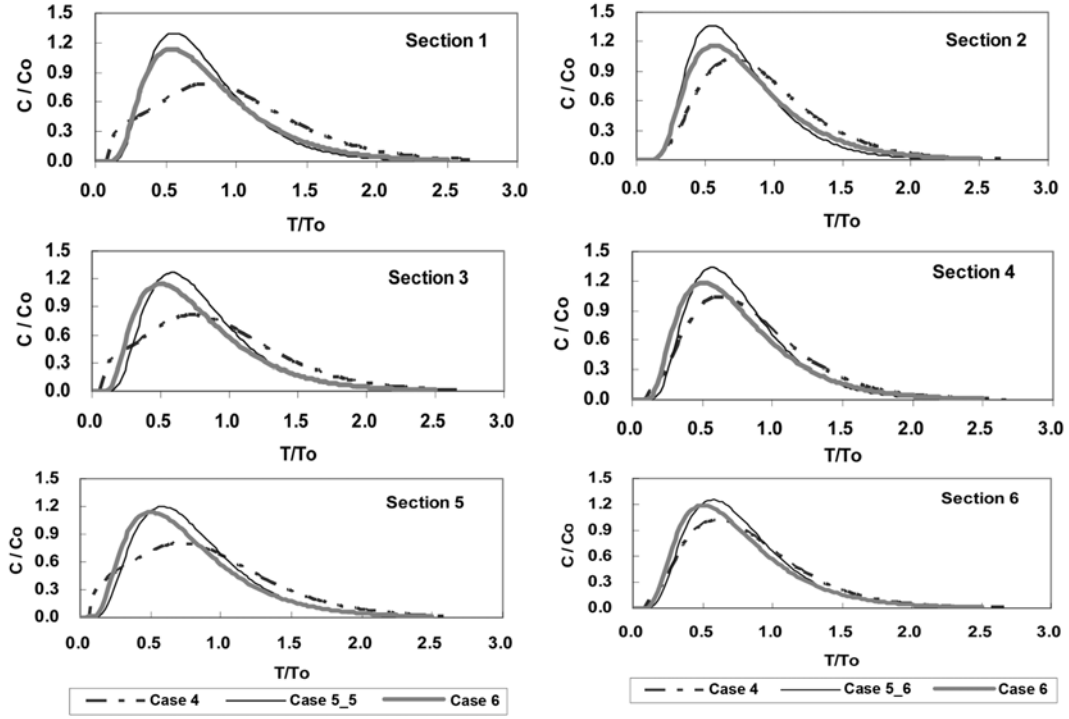

Fig. 10. Effluent concentration at the each sections of cases 4, 5 and 6: Sections 1, 2, 3, 4, 5, 6.

Table 4. Effluent flux (%) at the top, middle and bottom of cases 4, 5, 6

Section case	Top		Middle		Bottom	
	1	2	3	4	5	6
Case 4	16.6	17.8	15.9	17.2	15.7	16.8
Case 5	15.5	15.7	16.2	16.1	18.9	17.6
Case 6	16.7	18.0	15.8	17.0	15.8	16.7

than those of other cases. In contrast, the Tp index indicating the peak time of the species is higher than other cases. So the values of the Morill dispersion index, indicating the mixing degree, are higher for cases 2, 3 and 4, including the square type, than those of other cases. The modal index is slightly higher for the cases that include a square type than for other cases. But the difference of the Morill and modal index for each case is very little. In the case of the short circuiting index, the values for the cases consisting of a square type are lower than those for cases consisting of a perforated baffle type. As mentioned above, the square type causes more short circuiting flow and is less effective for uniform flow than the perforated baffle. Therefore, the perforated baffle is more successful for uniform flow than the square type, and the third party wall of the flocculation process is significantly influential for the water flow distribution of the three party walls.

In addition, when comparing the cases that have a downward rectangular type (cases 1, 2, 3) and a perforated baffle type (cases 4, 5, 6) party wall at the final outlet, the downward rectangular type causes a bottom flow in the sedimentation basin due to the outlet of the final wall facing the bottom. The downward rectangular type is therefore unfavorable for retention time and capacity efficiency because the upper part of the sedimentation basin is seldom used for the settling process, and it can also be a cause of decreasing sedimentation efficiency. Although originally the purpose of using the downward square type as the final outlet wall was to consider the case of high turbidity, there are only a few days (less than 30) when the turbidity of the Nakdong River water entering the drinking water treatment system exceeds 50 NTU. Therefore, it can be considered that the perforated baffle is more desirable for the final outlet of the flocculation process than the downward rectangular

Table 5. The index of cases 1, 2, 3, 4, 5, 6

Index case	1	2	3	4	5	6	Remark
T10 (min)	19.6	15.3	14.5	18.3	18.5	17.3	10% Overflow time
T90 (min)	62.2	65.0	66.8	76.0	62.8	66.6	90% Overflow time
Tp (min)	29.2	29.6	29.9	34.0	27.2	26.0	Peak time
Morill	3.18	4.25	4.62	4.17	3.40	3.85	PFR=1, CSTR>>1, T90/T10
Modal	0.58	0.59	0.60	0.68	0.54	0.52	Plug flow=1 (Tp/T), T (HRT)=50 min
Short circuiting	0.39	0.31	0.29	0.37	0.37	0.35	Short circuiting<<1, (T10/T)

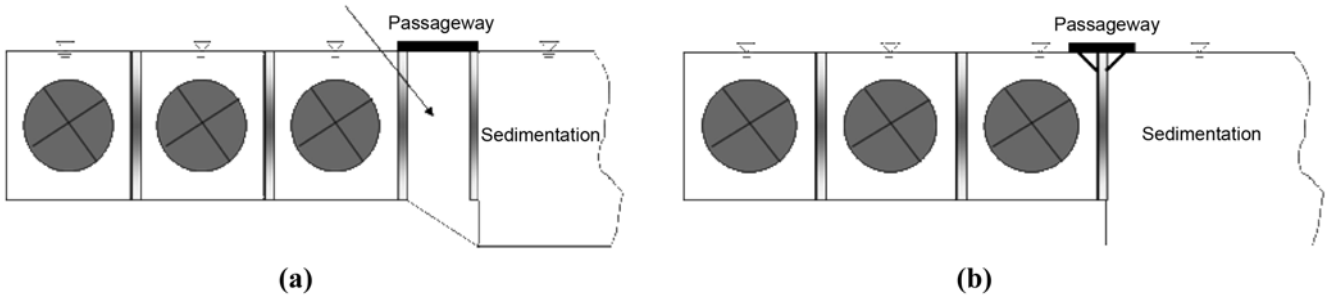

Fig. 11. A cross section of flocculation basin: (a) A present flocculation basin, (b) A suggested flocculation basin.

type.

Generally, in Korea, four party walls are used in flocculation basins: three party walls and a final outlet wall. The space between the third party wall and the final outlet wall is not included in the flocculation basin and sedimentation basin. This boundary is shown by an arrow, ↘, in Fig. 11(a). The top of this space is covered with concrete and is used as a passageway. Because there is no flocculator at this space, the formed flocs are settled. Therefore, as the time goes on, the flocs accumulate on the bottom of the flocculation basin. In addition, accumulated flocs fill up the hole of the outlet wall, causing an upward effluent at the outlet wall. However, the accumulated flocs can only be removed by cleaning the flocculation basin every year. We therefore suggest the removal of any one of both the third party walls and the final outlet wall in order to prevent the settlement of the flocs at this space. This is shown in Fig. 9(b). In order to achieve a practical application of the third party wall as an outlet wall, additional studies are required on the volume capacity of the third flocculation process. At the present, to improve the operating efficiency of the flocculation basin, the pillar type is suitable as a third wall. Therefore, case 6 holds outstanding output out of the six cases tested in this study.

CONCLUSION

Simulation using CFD software was conducted in order to evaluate flow characteristics according to party wall type. Conclusions are made as follows:

The perforated baffle type is more effective for uniform flow than the square type, and the third party wall of the flocculation process has the most influence of the three party walls for water flow distribution.

To prevent sinking of the flocs formed between the third party wall and the final outlet wall, it is necessary to develop the third party wall into an actual final outlet wall or to modify it into a pillar baffle type.

To achieve the practical application of a third party wall as a final outlet wall, additional studies on the volume capacity of the third flocculation process as well as the opening ratio of the perforated baffle are required in order to minimize the eddies in the flocculation process and to reduce kinetic energy for a stable sedimentation process.

In the case of a drinking water treatment system that treats low density water, a perforated baffle is more efficient as a final outlet wall because a downward rectangular type may form a bottom flow, which may cause a reduction in the efficiency of the volume capacity.

REFERENCES

1. Y. J. Jung and K. S. Min, *J. Korean Society on Water Quality*, **21**, 230 (2005).
2. Prabhata, K. Swamee and A. Tyagi, *ASCE*, **122**, 71 (1996).
3. P. Larwen, Report No. 1001, University of Lund, Lund, Sweden (1997).
4. P. Krebs, *Water Sci. Technol*., **31**, 181 (1995).
5. J. M. Kim and G. Y. Han, *Korean J. Chem. Eng*., **24**, 445 (2007).
6. A. Cockx, Z. Do-quang, A. Line and M. Roustan, *Chem. Eng. Sci*., **54**, 5085 (1999).
7. H. Wang and R. A. Falconer, *Water Res*., **32**, 1529 (1998).
8. J. Zhang, P. M. Huck, G. D. Stubley and W. B. Anderson, *AQUA*, **57**, 79 (2008).
9. G. Mazzolani, F. Pirozzi and G. d'Antonoi, *Water Sci. Tech.*, **38**, 95 (1998).
10. Copyright by Fluent Inc., FLUENT6.3 User's Guide, **3**, 14.1 (2006).
11. G. A. Ekama, J. L. Barnard, P. Krebs and J. A. McCorquofale, *JAWQ*, **173** (1997).
12. J. Bridgeman, B. Jefferson and S. A. Parsons, *Advances in Eng. Software*, **21** (2009).
13. R. Dupont and C. Dahl, *Water Sci. Tech.*, **31**, 215 (1995).
14. Bishop, M. Mark, J. M. Morgan, B. Comwell and D. K. Jamison, *AWWA*, **85**, 68 (1993).
15. John Bridgeman, Bruce Jefferson and Simon Parsons, *Chem. Eng. Sci. Design*, **86**, 941 (2008).
16. N. S. Park, H. K. Park and H. W. Ahn, *J. Korean Society of Water and Wastewater*, **18**(3), 291 (2004).
17. A. I. Stamou, *Applied Mathematical Modelling*, **15**(7), 351 (1991).